CHAPTER 5

MELT RHEOLOGICAL BEHAVIOUR OF NBR/EVA BLENDS

The results of this chapter have been accepted for publication in *Polym.-Plast. Technol. Eng.*

Melt rheological studies are useful for optimising processing conditions and understanding the effect of various parameters on flow behaviour of materials. It is also possible to make a rational selection of the best polymer or polymer component to be used under a given set of conditions.[1] Thus, a thorough knowledge of the melt viscosity, elasticity and extrudate characteristics of polymer melts is of great importance in polymer processing.

Danesi *et al.*[2] have attempted to clarify the influence of such compositional variables as molecular weight, chemical affinity and blend composition on the extrudate morphology of isotactic polypropylene/ethylene-propylene rubber blends. Goettler *et al.*[3] have interpreted the rheology of olefinic thermoplastic vulcanisates in terms of a simple morphological model. Rheological studies on binary and ternary blends of PP, ABS and LDPE were reported by Gupta *et al.*[4] Recently Koshy *et al.*[5] have reported the stratification and particle breakdown during the extrusion of NR/EVA blends with respect to blend ratio and shear rate. A rheological evaluation of blends of PC/LLDPE[6] and PS/PE[7] was carried out by Utracki *et al.*

This chapter deals with the melt viscosity, melt elasticity, extrudate characteristics and morphology of NBR/EVA blends as a function of blend composition, crosslinking system and shear rate.

5.1 Results and discussion

5.1.1 Melt viscosity

The dependence of viscosity on shear stress of various blend compositions for uncrosslinked NBR/EVA blends at 90°C is shown in Figure 5.1. It can be seen that the viscosity of all the blends decreases with the increase in shear stress indicating pseudoplastic behaviour. The pseudoplastic behaviour is due to the orientation and disentanglement of polymer chains under the application of shear force. At zero shear, the molecules are randomly oriented and extensively entangled. Hence higher viscosities are observed at lower shear. For a given shear stress the viscosity of NBR is slightly higher than that of EVA.

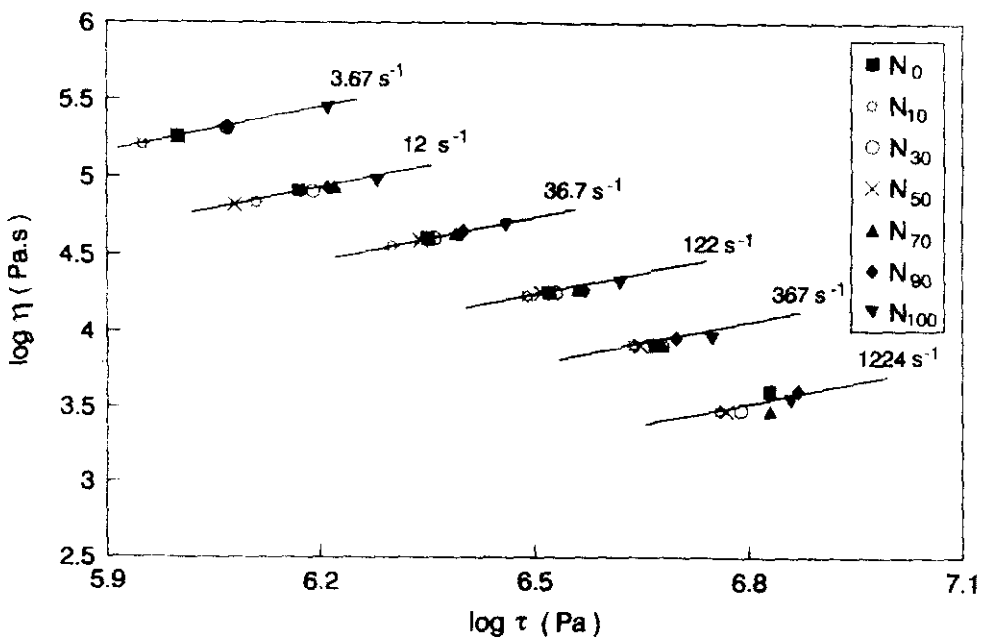

Figure 5.1. The dependence of viscosity on shear stress of uncrosslinked NBR/EVA blends at 90°C

The variation of viscosity with the weight percentage of NBR at low, medium and high shear rates is presented in Figure 5.2. In the case of blends the viscosity values show negative deviation from the additivity line. The negative

deviation is associated with the interlayer slip between the immiscible components of the blend.[8] NBR/EVA system exhibits a two phase morphology and hence a negative deviation from the additivity line. This type of negative deviation was reported by many researchers.[8-11] Varkey *et al.*[8] have reported a drastic reduction in the viscosity of NR on addition of ENR in the NR/ENR latex blends. In the case of polyacetal/PMMA system, the negative deviation in viscosity becomes less visible at high shear rates.[11]

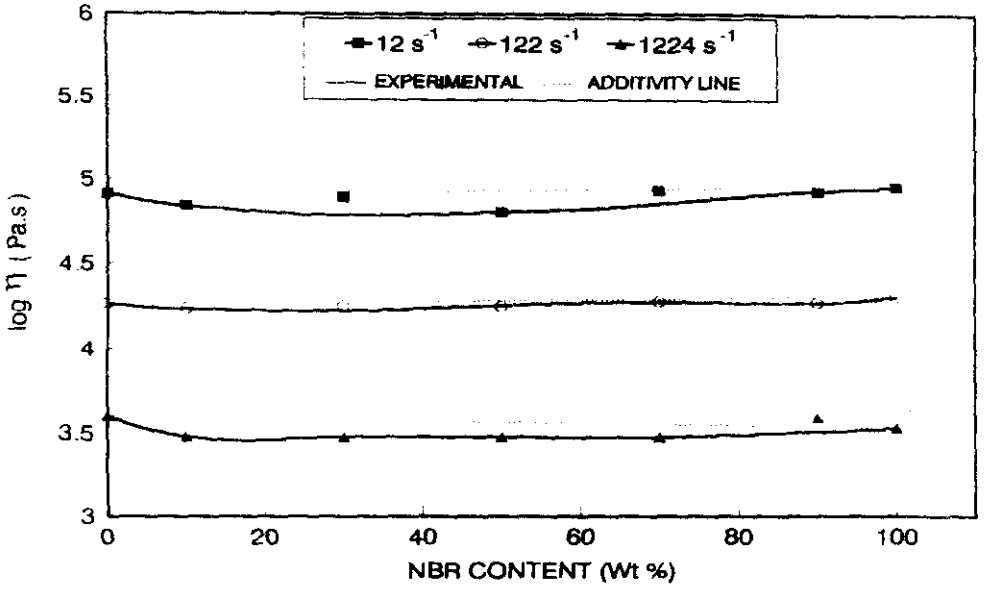

Figure 5.2. The variation of viscosity with the weight percentage of NBR at different shear rates

Utracki and Sammut[7] showed that positive or negative deviation of measured viscosity from that calculated based on the log additivity rule is an indication of strong or weak interactions between the phases of the blend. According to them,

$$\ln (\eta_{app})_{blend} = \sum_i w_i \ln (\eta_{app})_i \qquad (5.1)$$

where w_i is the weight fraction of the i^{th} component of the blend and η_{app} is the apparent viscosity. They indicated that immiscible blends show negative deviation due to heterogeneous nature of the components whereas positive deviation is

expected for blends due to high solubility and homogeneous nature of the components.[7] The following models are used to calculate the viscosity of NBR/EVA blends at shear rate of 36.7 s^{-1}. According to the rule of additivity,

$$\eta = \eta_1\phi_1 + \eta_2\phi_2 \qquad \text{(Model I)} \qquad (5.2)$$

where η_1 and η_2 are the viscosities of the components and ϕ_1 and ϕ_2 are their volume fractions.

Viscosity can also be calculated using Hashin's upper and lower limit models [12]

$$\eta_{max} = \eta_2 + \frac{\phi_1}{1/(\eta_1 - \eta_2) + \phi_2/2\eta_2} \qquad \text{(Model II)} \qquad (5.3)$$

$$\eta_{max} = \eta_1 + \frac{\phi_2}{1/(\eta_2 - \eta_1) + \phi_1/2\eta_1} \qquad \text{(Model III)} \qquad (5.4)$$

η_1, η_2, ϕ_1 and ϕ_2 have the same significance as before.

From the theoretical modelling it is found that the melt viscosity of NBR/EVA blends calculated using all the models show a deviation from the experimental value (Figure 5.3). The negative deviation of the experimental value can be attributed to the heterogeneous nature of the blend.

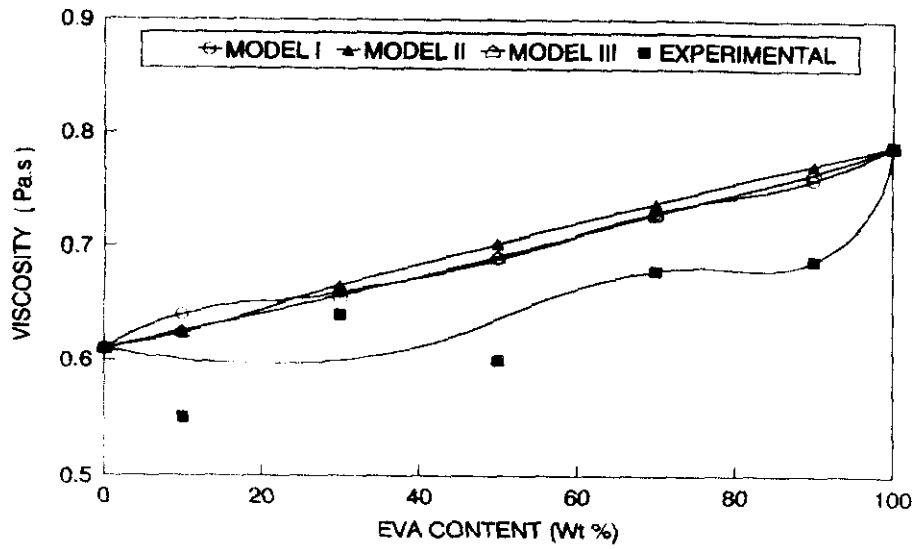

Figure 5.3. Theoretical modelling to predict the melt viscosity of NBR/EVA blends

The dependence of viscosity of NBR/EVA blends on shear stress of the uncrosslinked and the three crosslinking systems, namely, peroxide, sulphur and mixed system is shown in Figure 5.4. Since the measurements are made at 90°C, no crosslinking is expected to take place during extrusion. Therefore, the flow behaviour of these compounds is similar to that of the unvulcanised system (N_{30}). However, slight variations are observed in certain cases due to the presence of compounding ingredients. Similar behaviour was observed by Koshy *et al.*[13] in the case of NR/EVA blends in presence of compounding ingredients.

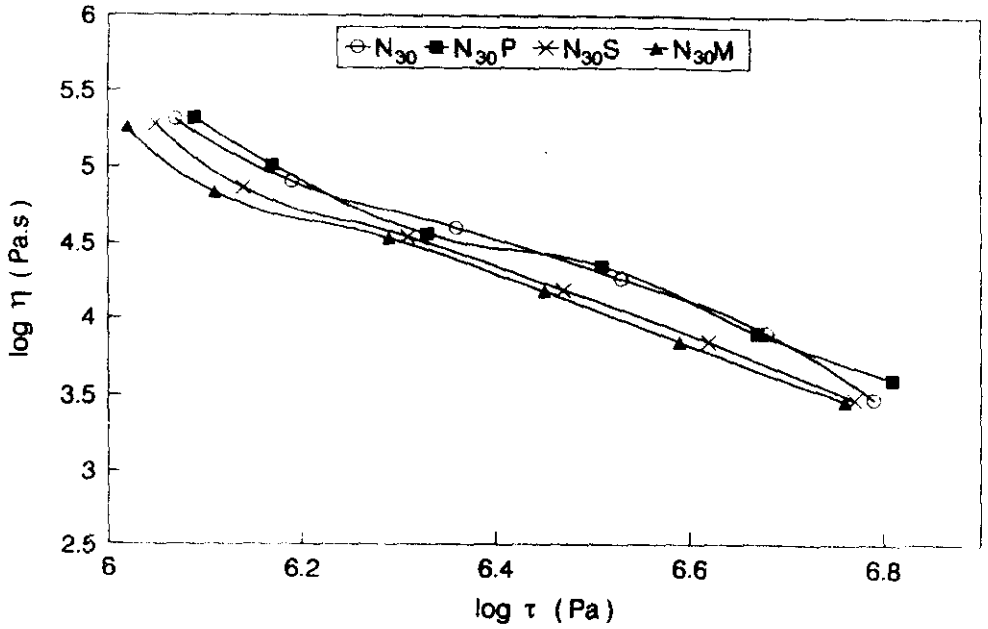

Figure 5.4. The dependence of viscosity on shear stress for various crosslinking systems of NBR/EVA blends

The effect of blend ratio on the flow behaviour indices of the samples is given in Table 5.1. Pseudoplastic materials are characterised by n' below 1. In the case of uncrosslinked blends the n' value increases as the proportion of EVA in the blend increases. Therefore it can be concluded that blends with high EVA content

are less pseudoplastic than blends with low EVA content. From the Table 5.1 it may be inferred that the crosslinking systems show little effect on the flow behaviour index of NBR/EVA blends.

Table 5.1 Flow behaviour index of NBR/EVA blends

Sample reference	Flow behaviour index (n')			
	Blend	DCP (P)	Sulphur (S)	Mixed (M)
N_0	0.33	0.29	-	0.30
N_{30}	0.29	0.30	0.29	0.30
N_{50}	0.32	0.33	0.33	0.33
N_{70}	0.29	0.31	0.31	0.32
N_{100}	0.27	-	0.33	0.33

5.1.2 Melt elasticity

Properties characterising the elasticity of polymer melts are die swell, principal normal stress difference ($\tau_{11}-\tau_{22}$), recoverable shear strain (S_R) and elastic shear modulus (G).

The principal normal stress difference ($\tau_{11}-\tau_{22}$) is calculated from the die swell and shear stress according to Tanner's equation,[14]

$$\tau_{11}-\tau_{22} = 2\,\tau_w\,[2(d_e/d_c)^6-2]^{1/2} \qquad (5.5)$$

Recoverable shear strain (S_R) and the apparent shear modulus (G) are calculated from the following equations,

$$S_R = (\tau_{11}-\tau_{22})/2\tau_w \qquad (5.6)$$

$$G = \tau_w/S_R \qquad (5.7)$$

The principal normal stress difference ($\tau_{11}-\tau_{22}$), elastic shear modulus (G) and recoverable elastic shear strain (S_R) of NBR/EVA blends at a shear rate of 36.7 s^{-1} are given in Table 5.2. A high value of $\tau_{11}-\tau_{22}$ implies higher elasticity of the material

Figure 5.5 represents the variation of principal normal stress difference and shear stress with shear rate. It is clear from the figure that the magnitude of principal normal stress difference ($\tau_{11}-\tau_{22}$) is much higher than that of the shear stress (τ_w) for all the samples. The variation of elastic shear modulus (G) and recoverable elastic shear strain (S_R) with shear rate is given in Figure 5.6. As the shear rate increases, an increase in the elastic shear modulus is observed. The S_R values show an initial increase with shear rate, reaches a maximum and then decreases with further increase in shear rate.

Table 5.2. Melt elasticity of NBR/EVA blends extruded at 90°C at a shear rate of 36.7 s^{-1}

Sample reference	Parameters		
	$\tau_{11}-\tau_{22} \times 10^5$ (Pa)	G $\times 10^5$ (Pa)	S_R
N_0	183	5.50	4.07
N_{10}	152	5.28	3.79
N_{30}	178	6.18	3.79
N_{50}	129	7.55	2.92
N_{70}	151	8.34	3.01
N_{90}	156	8.18	3.09
N_{100}	249	6.85	4.26

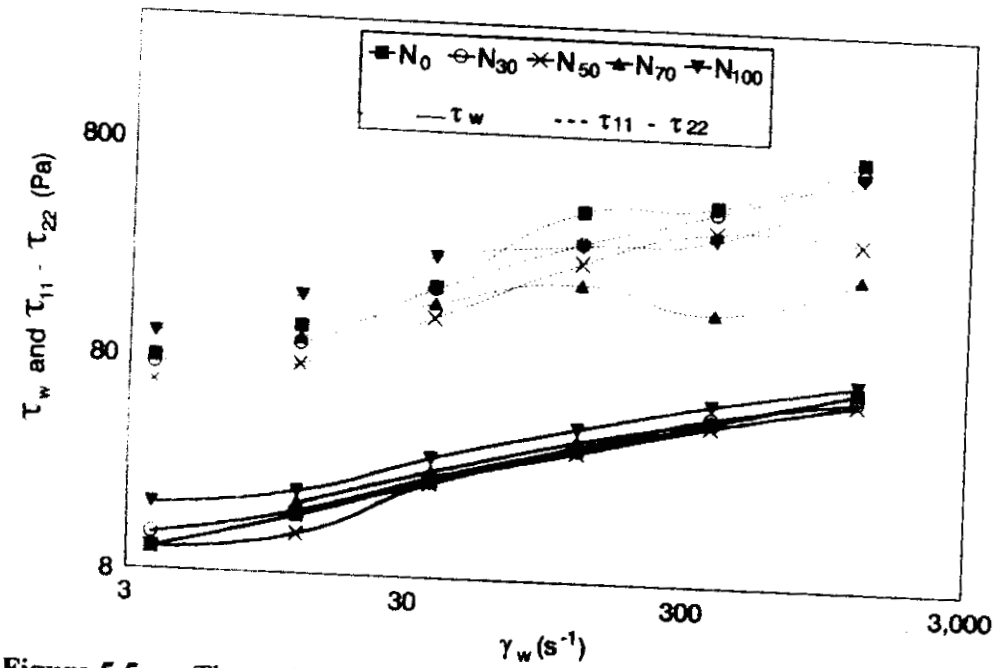

Figure 5.5. The variation of shear stress and principal normal stress difference with shear rate of NBR/EVA blends

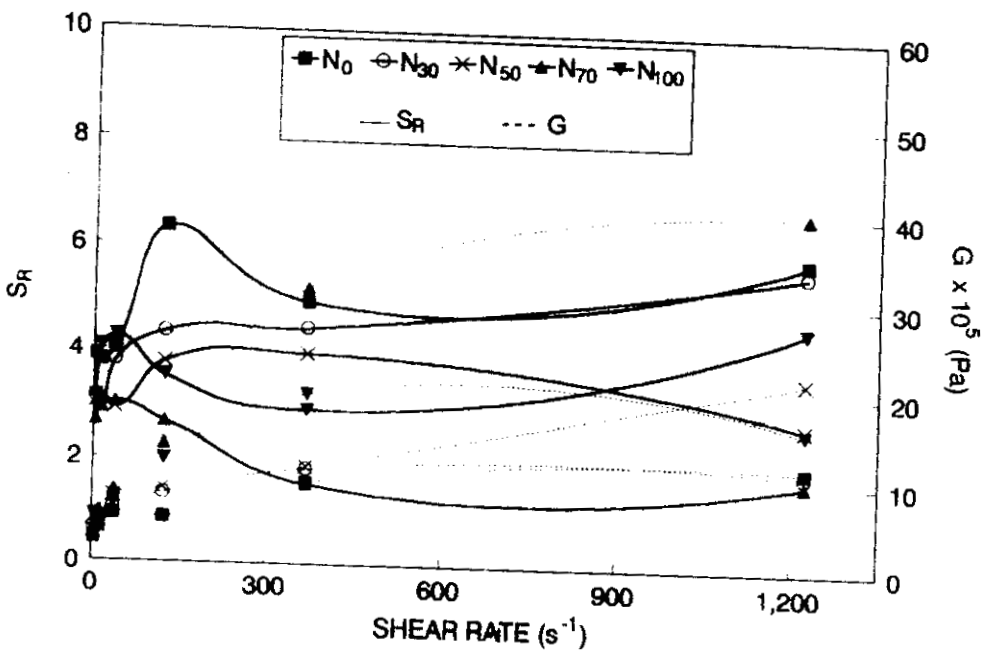

Figure 5.6. The variation of recoverable elastic shear strain and elastic shear modulus with shear rate

5.1.3 *Die swell*

When a molten polymer flows through a capillary the polymer chains get oriented due to shear. On emerging from the capillary into the atmosphere, recoiling of polymer chains takes place, the contraction in the direction of flow being offset by lateral expansion, resulting in the phenomenon of die swell or extrudate swell. Factors controlling elastic recovery are crosslinking, chain branching, stress relaxation and the presence of fillers and plasticizers. The die swell values of NBR/EVA blends are given in Table 5.3. EVA has lower die swell than NBR. The variation in die swell with shear rate is also noted. At high shear rates pressure exerted on the material is high. Therefore the material has higher elastic recovery. This leads to higher die swell. Hence usually the die swell increases with increasing shear rate.

Table 5.3. Die swell of NBR/EVA blends

Sample reference	Shear rate (s^{-1})	
	12	36
N_0	1.42	1.45
N_{10}	1.36	1.42
N_{30}	1.33	1.42
N_{50}	1.34	1.32
N_{70}	1.32	1.33
N_{90}	1.41	1.34
N_{100}	1.45	1.47

The effect of blend composition on shear rate of the blends is shown in Figure 5.7. Here the die swell is plotted against shear rate and it is observed that initially the die swell increases with increasing shear rate and after reaching a

critical shear rate it drops. This critical shear rate varies with blend composition. Pure EVA and blends with a high EVA content, where EVA forms the continuous phase, exhibit a higher critical shear rate at 367 s^{-1}. For NBR and blends with a high NBR content, the critical shear rate is found to be 36.7 s^{-1}. The lower value is due to the phase inversion in morphology of the system beyond N_{50} where nitrile rubber is the continuous phase.

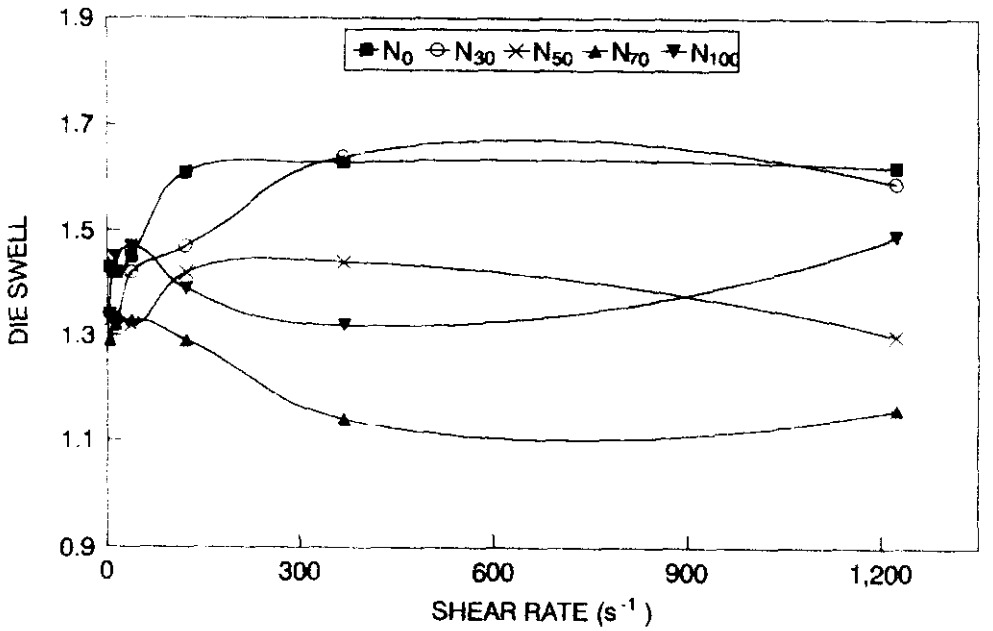

Figure 5.7. The dependence of die swell on shear rate and blend composition of NBR/EVA blends

5.1.4 Extrudate deformation

Figure 5.8 shows the photograph of the blends extruded at three different shear rates. At low shear rates, most of the extrudates have smooth surfaces. However, at higher shear rates the extrudate surfaces exhibit distortion. The extent of distortion increases with increase in shear rate. The extrudate at a shear rate of 122 s^{-1} exhibits a rough surface. The surface roughness is further increased in the

case of the extrudates at a shear rate of 1224 s^{-1}. This is associated with the melt fracture that occurs at high shear forces where the shear stress exceeds the strength of the melt.

BLEND COMPOSITION	SHEAR RATE (s^{-1})		
	12	122	1224
N_0	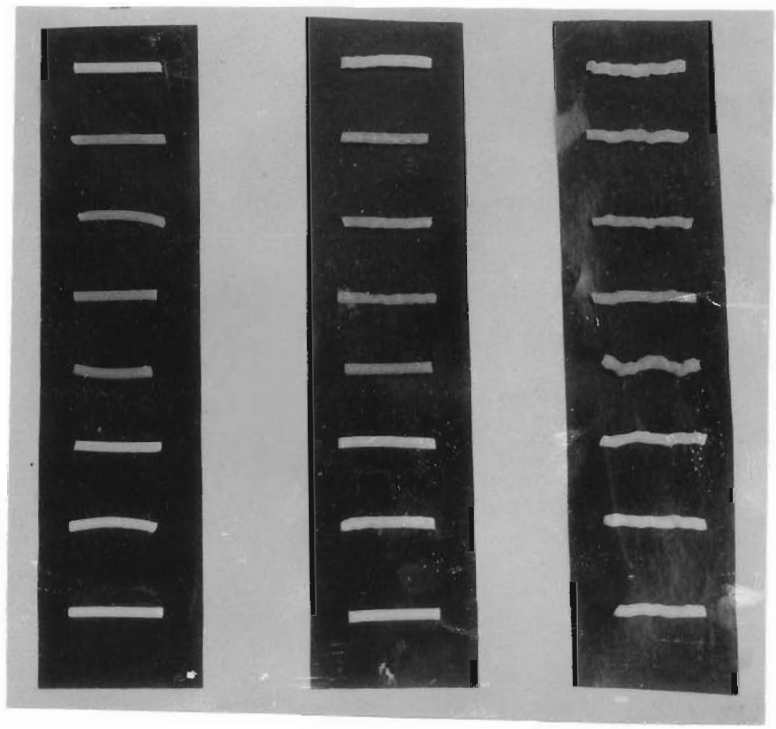		
N_{30}			
N_{50}			
N_{70}			
N_{100}			
$N_{30}P$			
$N_{30}S$			
$N_{30}M$			

Figure 5.8. Photograph of NBR/EVA blends extruded at different shear rates

5.1.5 Morphology of the extrudates

Micrographs of the extrudate of N_{30} obtained at different shear rates are shown in Figure 5.9. From the micrographs it is clear that the domain size decreases with increasing shear rate. However, at higher shear rate (Figure 5.9c) a

few larger domains are observed due to the recombination of particles under the high shearing force.

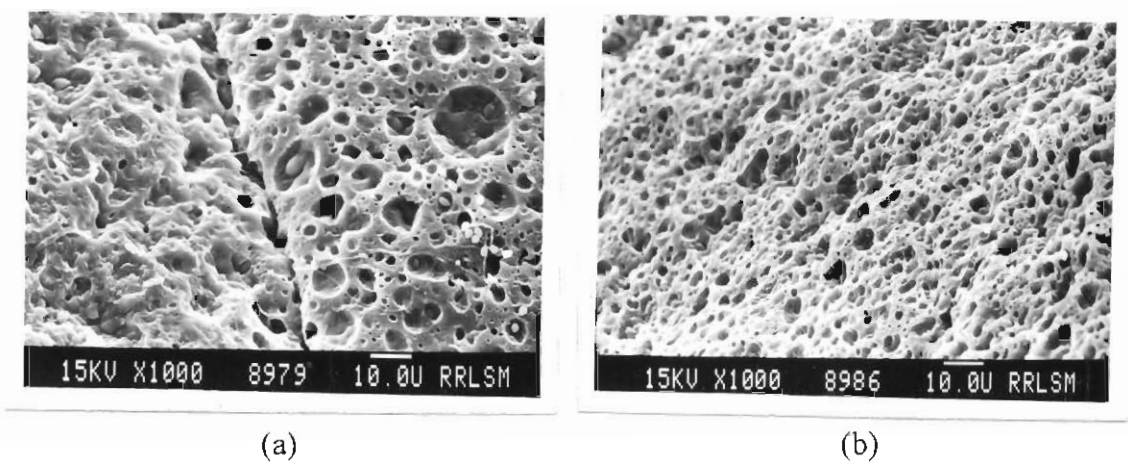

(a) (b)

(c)

Figure 5.9. Scanning electron micrographs of the extrudates of N_{30} obtained at shear rates of (a) 12 s^{-1}, (b) 122 s^{-1} and (c) 367 s^{-1}

Generally a decrease in particle size is observed with an increase in shear rate. A schematic representation of this is given in Figure 5.10. The decrease in particle size with the increase in shear rate is due to the deformation and consequent breakdown of particles in the capillary under the action of shear force.

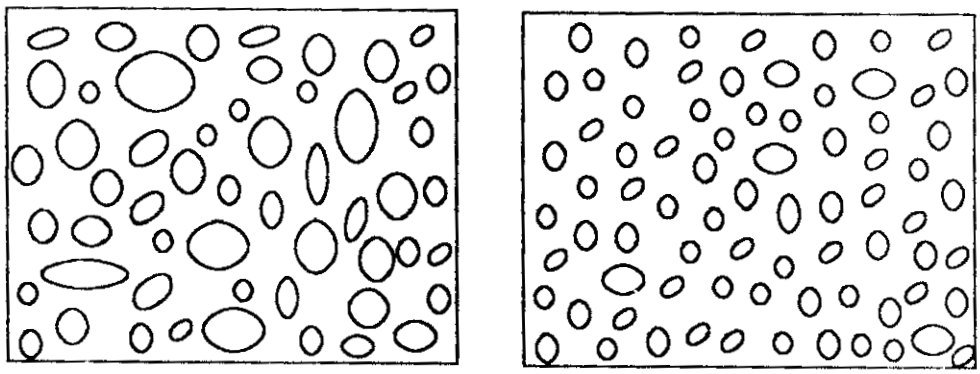

Figure 5.10. Schematic representation of the morphology at (a) low shear rate and (b) high shear rate.

The particle size distribution curve (Figure 5.11) at different shear rates also indicates a finer dispersion of the domains at high shear rates. The distribution curve at 12.24 s^{-1} is broad indicating a high degree of polydispersity. As the shear rate increases the distribution curve becomes narrow due to the uniform distribution of the dispersed phase.

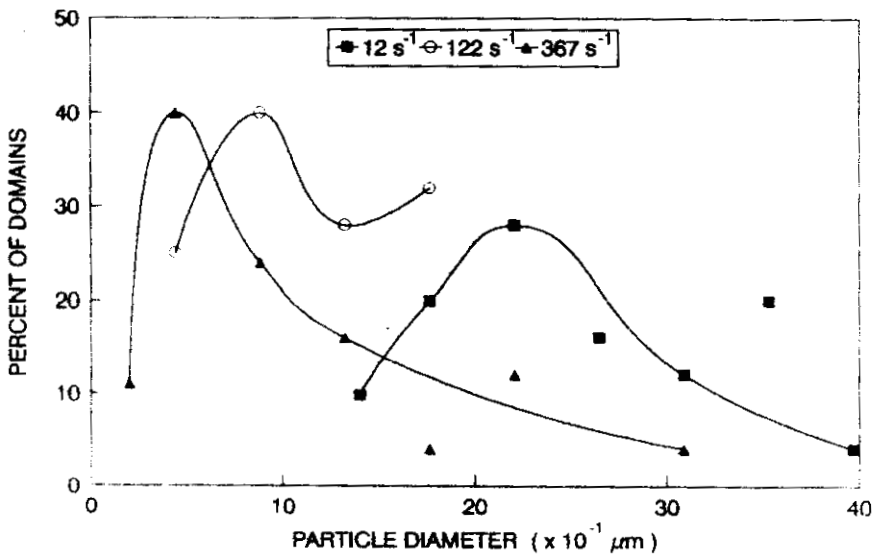

Figure 5.11. The particle size distribution curve at different shear rates

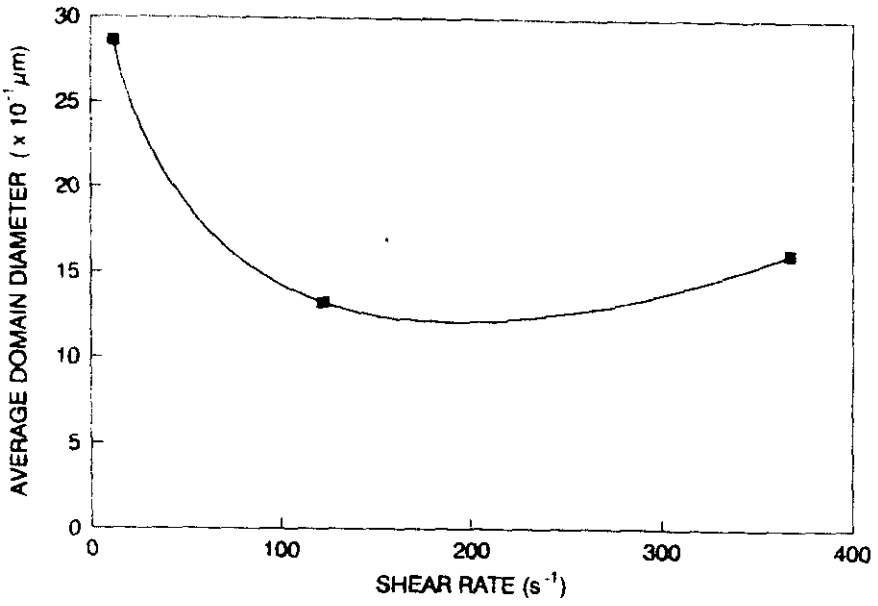

Figure 5.12. The dependence of average domain diameter on shear rate

The average domain diameter versus shear rate is plotted in Figure 5.12. The average domain diameter decreases as the shear rate increases from 12 to 122 s^{-1}. But at a higher shear rate of 367 s^{-1} there is a slight increase in average domain diameter. This is due to the coalescence of the dispersed domains under the high shearing force.

In order to study the effect of blend composition on the extrudate morphology, the extrudates at a shear rate of 367 s^{-1} are observed under the scanning electron microscope (Figure 5.13). In N_{30} (Figure 5.13a), NBR is the dispersed phase, N_{50} (Figure 5.13b) exhibits a co-continuous morphology and in N_{70} (Figure 5.13c) EVA forms the dispersed phase. Morphology of the extrudates and cryogenically fractured surface is similar (Figure 3.2). Figure 5.13d is the scanning electron micrograph of the core region of N_{70}. From the micrograph it is clear that the stratification phenomena, i.e., the segregation of the blend components to core and periphery does not exist in this system. This is due to the matching in the viscosities of the two components.

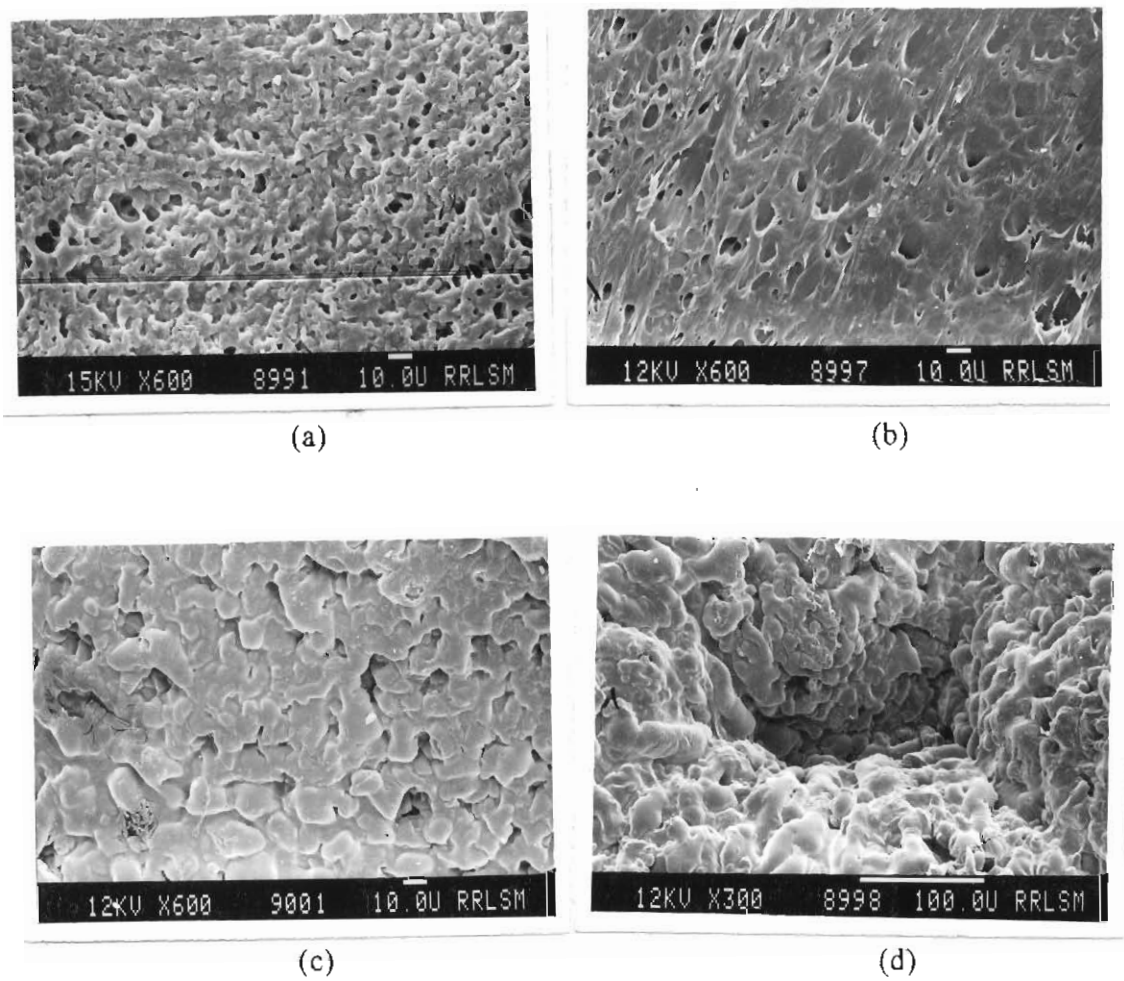

Figure 5.13. Scanning electron micrographs of extrudate at a shear rate of 367 s^{-1} (a) N_{30}, (b) N_{50}, (c) N_{70} and (d) core region of N_{70}

5.2 References

1. J. A. Brydson, *Flow Properties of Polymer Melts*, George Godwin Ltd., London, 1981.
2. S. Danesi and R. S. Porter, *Polymer*, **19**, 448 (1978).
3. L. A. Goettler, J. R. Richwine and F. J. Wille, *Meeting of Rubber Division*, American Chemical Society, Philadelphia, Pennsylvania, May 4-7, 1982.
4. A. K. Gupta, A. K. Jain and S. N. Maiti, *J. Appl. Polym. Sci.*, **38**, 1699 (1989).
5. A. T. Koshy, S. Thomas and B. Kuriakose, *Kauts. Gummi Kunsts.*, **47**, 108 (1994).

6. L. A. Utracki and P. Sammut, *Polym. Eng. Sci.*, **30**, 1027 (1990).

7. L. A. Utracki and P. Sammut, *Polym. Eng. Sci.*, **28**, 1405 (1988).

8 J. T Varkey, S. S. Rao and S. Thomas, *Polym. Plast. Technol. Eng.*, **35**, 1 (1996).

9. C. K. Shah, *Polym. Eng. Sci.*, **16**, 742 (1976).

10. C. D. Han and Y. W. Kim, *J. Appl. Polym. Sci.*, **19**, 2831 (1975).

11 J. F. Carley, *Reprints STP Reg. Conf. on Plast. Progr. Proc.*, 285 (1980).

12 S. Akhtar, B. Kuriakose, P. P. De and S. K. De, *Plast. Rubber Process. Appln.*, **7**, 11 (1987).

13 A. T. Koshy, B. Kuriakose, S. Thomas, C. K. Premalatha and S. Varghese, *J. Appl. Polym. Sci.*, **49**, 901 (1993).

14. R. I. Tanner, *J. Polym. Sci., A-Z*, **14**, 2067 (1970).